# Nonlinear finite element modelling of RC members under static load using ABAQUS

Sampa Akter[1] and Tahsin Reza Hossain[2]

[1]*Department of Civil Engineering*
*Military Institute of Science and Technology, Dhaka*
[2]*Department of Civil Engineering*
*Bangladesh University of Engineering and Technology, Dhaka*

**Abstract**

Due to difficulties and high costs of experimental research, numerical studies can be an appropriate alternative for experimental methods. in this current research capability of the finite element method for predicting concrete behaviour under static loading conditions is evaluated using explicit dynamic analysis in ABAQUS (2014). The concrete damaged–plasticity (CDP) model proposed by Lubliner and collaborators is employed herein for the plain concrete, and elasto-plastic material models are employed for the steel reinforcement. A perfect bond is assumed between the reinforcements and concrete, whereby the bond–slip behaviour, as well as damage along crack patterns, are modelled through concrete damage. First, the proposed method is presented and then is validated. The proposed methodology has a wide range of applicability, and displays fast solution time while providing extensive and accurate information on structural behaviour. A high level of accuracy is demonstrated in various comparisons between analytical or test and analysis results of load displacement, crack patterns, failure type when subjected to static or monotonic loading.

*Keywords:* FEM, CDP, elasto-plastic, RC members, static load, validation.

## 1.     Introduction

Finite element method (FEM) is a computational approach which is considered to determine the approximate solutions of boundary value problems (Hutton and Wu, 2004). Finite element (FE) method is one of the most widely used methods in structural engineering whose ability and application have been studied for many years. Buyukozturk (1977) was one of the first researchers to develop a method to consider the effect of reinforcements on the finite element analysis of concrete structures. Then, several mathematical models to simulate the material and also interactive behaviors as the sources of nonlinearities in concrete structures for FEM analysis were extended (Vecchio 1989). Reinforced Concrete (RC) is a widely used construction material for structures such as tall buildings, bridges, tunnels, dams and military

shelters are built with RC elements. Studying the behavior of RC members under static load still is a fundamental research issue in the field of structural engineering. Experimental testing and numerical modelling of RC elements are always important to the researchers. The past studies on the RC members under static or monotonic loading indicate that most of previous researches have been carried out either experimentally or modeled numerically or in some cases both the approaches have been followed side by side. Since experimental testing is time-consuming and expensive, numerical approach like finite element (FE) simulations can be a valuable alternative method for experimental tests. Due to the complexity of the behavior and the nature of RC members, determination of the capable finite element model which can predict and calculate the exact responses is very difficult. There are several parameters that affect the analysis results of any RC member. Many studies exist (Zhang et al. 2016, Tong et al. 2017 and Richard et al. 2015) about the role of each of these parameters.

Therefore, proposing a comprehensive FE method which is accurate and simple is the main aim of this study. To reach this goal, numerical study of RC members like beam, column and frame are done against static and monotonic loading condition. A reliable finite element (FE) modelling of RC beam and column is developed and analyzed using ABAQUS (2014). However, to confirm the reliability of material models and the overall performance of the numerical model selected for determining the response of a member, validation against experimental/analytical results is required. Hence, FE models are validated against the test data found from the recent works as well as analytical results found from different literature for static load. Initially, for FE validation of RC beams under static load, six different types of RC beam are considered. Three of these are validated against analytical results and rest three against the test results of Saatci (2007). Moreover, one column is validated against analytical results and a frame is validated against test results of Güner (2008).

## 2.        Finite element modelling

ABAQUS is a versatile powerful finite element software which is utilized for simulation of complicated static as well as dynamic phenomena. The basic difference between static and dynamic analysis is equilibrium of external and internal forces. Any dynamic analysis will become static analysis if inertia and damping forces of structure become close to zero. The inertia and damping force of any structure will become very small when the rate of displacement of structure is very small. Again, the rate of displacement will be very small if mass of structure is very high but the mass of structure is a part of external load. To avoid this extra self-weight problem, the structure should be modeled without gravity action. For quasi-static analysis, downward displacement is applied and mass scaling technique is used.

### 2.1        Analysis method

The equation of motion can be solved using ABAQUS (2014) by performing explicit or implicit analysis. Explicit analysis is the default option in ABAQUS (2014) and widely used as the implicit analysis approach is computationally expensive for problems that needs to be discretized into small finite elements. The biggest difference between the two procedures lies in the manner in which the nodal accelerations are computed. In the implicit procedure a set of linear equations is solved by a direct solution method. The computational cost of solving this set of equations is high when compared to the relatively low cost of the nodal calculations with the explicit method.

### 2.2        Element type

Three dimensional eight noded solid elements (C3D8R) was utilized for modelling of concrete. two noded truss elements (T3D2) was used in this study for simulation of rebar.

### 2.3     Concrete and rebar interaction

Full bond between the steel and concrete is achieved by embedded techniques. This technique allows the placement of the reinforcement in any layout such that the displacements of the reinforcing bars are compatible with those of the concrete element. The support and load are applied on beam or column by steel plate of 25 mm thickness. Contact between loading plate and solid concrete elements are achieved by using surface to surface contact (Explicit) algorithms using penalty method. The element size of 25 mm is used for modelling of concrete beam/column, reinforcement, steel supports and loading plate which are obtained from mesh sensibility analysis as discussed in following sections.

### 2.4     Material modeling

#### 2.4.1     Concrete

Concrete Damage Plasticity (CDP) model which was proposed by Lubliner et al. (1998) and elaborated by Lee and Fenves (1989), is used for simulation of concrete.

In Figure 1 (a), $\varepsilon_c^{ch}$ and $\varepsilon_{oc}^{ch}$ are the crushing and elastic undamaged components of strain; $\varepsilon_c^{pl}$ and $\varepsilon_c^{el}$ are the plastic and elastic damaged components. In Figure 1 (b), $\varepsilon_c^{ck}$ and $\varepsilon_{ot}^{el}$ are the cracking and elastic undamaged strain components; $\varepsilon_t^{pl}$ and $\varepsilon_t^{el}$ are the plastic and elastic damaged components.



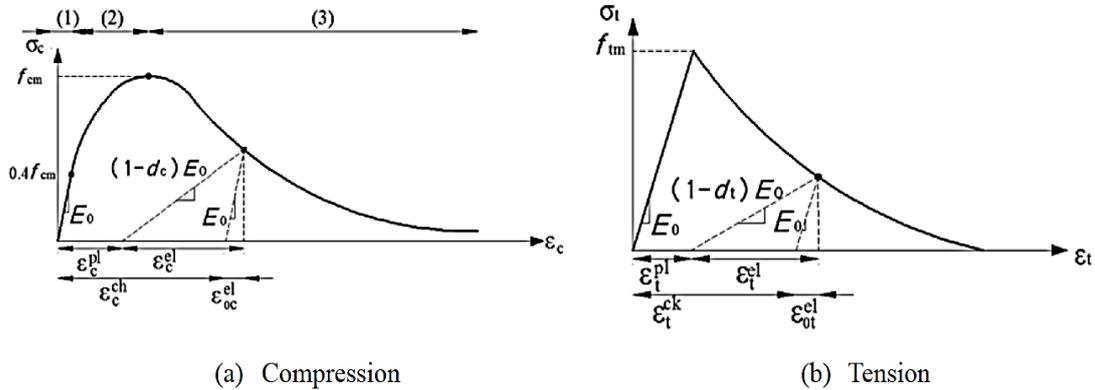(a)  Compression                                    (b)  Tension

Fig. 1.  Assumed uniaxial model of concrete behaviour (Lee and Fenves, 1998) (a) is linear, $\sigma_{c(1)} = E_0\varepsilon_c$, reaching $0.4f_{cm}$; second (ascending) segment (in between $0.4 f_{cm}$ and $f_{cm}$) is quadratic (CEB-FIP, 2010):

$$\sigma_{c(2)} = \frac{E_{ci}\frac{\varepsilon_c}{f_{cm}} - \left(\frac{\varepsilon_c}{\varepsilon_{cm}}\right)^2}{1 + \left(E_{ci}\frac{\varepsilon_{cm}}{f_{cm}} - 2\right)\frac{\varepsilon_c}{\varepsilon_{cm}}} f_{cm} \tag{1}$$

$E_{ci}$ is the modulus of deformation of concrete for zero stress, given by $E_{ci} = 10000 f_{cm}^{1/3}$ and $E_0 = (0.8 + 0.2 f_{cm}/88) E_{ci}$ (in MPa) (CEB-FIP, 2010). In the initial linear branch, $E_0$ is the secant modulus that corresponds to $0.4 f_{cm}$ stress. Third (descending) segment is given by:

$$\sigma_{c(3)} = \left(\frac{2 + \gamma_c f_{cm}\varepsilon_{cm}}{2f_{cm}} - \gamma_c\varepsilon_c + \frac{\varepsilon_c^2\gamma_c}{2\varepsilon_{cm}}\right)^{-1} \tag{2}$$

$$\gamma_c = \frac{\pi^2 f_{cm} \varepsilon_{cm}}{2\left[\frac{G_{ch}}{l_{eq}} - 0.5 f_{cm}\left(\varepsilon_{cm}(1-b) + b\frac{f_{cm}}{E_0}\right)\right]^2} \qquad b = \frac{\varepsilon_c^{pl}}{\varepsilon_c^{ch}} \qquad (3)$$

$G_{ch}$ is the crushing energy per unit area (Krätzig and Pölling, 2004) and $l_{eq}$ is the characteristic length, which depends on the mesh size, the type of finite element and the crack direction. Based on experimental observations, $b = 0.9$ can be initially assumed. After calculating the damage variables, the average value of $b$ is obtained.

Regarding tensile behaviour, the ratio between tensile stress $\sigma_{t(w)}$ (for crack width $w$) and maximum tensile strength $f_{tm}$, is given by (Hordijk 1992):

$$\frac{\sigma_{t(w)}}{f_{tm}} = \left[1 + \left(c_1 \frac{w}{w_c}\right)^3\right] e^{-c_2 \frac{w}{w_c}} - \frac{w}{w_c}(1 + c_1^3)e^{-c_2} \qquad (4)$$

In Eq. (4), $c_1 = 3$, $c_2 = 6.93$ (Hordijk, 1992), and $w_c$ is the critical crack opening. Eq. (5) shows that $\sigma_t(0) = f_{tm}$ and $\sigma_{t(wc)} = 0$. Therefore, $w_c$ can be considered as the fracture crack opening. Eq. (5) (Hordijk, 1992) relates $w_c$ with the tensile strength and fracture energy $G_F$ per unit area:

$$w_c = 5.14 G_F / f_{tm} \qquad (5)$$

According to CEB-FIP (2010), $G_F$ (N/mm) can be calculated as

$$G_F = 0.073 f_{cm}^{0.18} \qquad (6)$$

In Eq. (6), $f_{cm}$ is expressed in MPa. The ratio between crushing and fracture energies can be assumed proportional to square of the ratio between compressive and tensile strengths (Oller, 1988):

$$G_{ch} = \left(\frac{f_{cm}}{f_{tm}}\right)^2 G_F \qquad (7)$$

In the descending segment of the tensile stress-strain curve as shown in Figure 1(b), the strain can be obtained in terms of the crack opening from the following kinematic relation:

$$\varepsilon_t = \varepsilon_{tm} + w/l_{eq} \qquad (8)$$

Tensile and compressive damage functions are derived as follows:

$$d_c = 1 - \frac{1}{2 + a_c}\left[2(1 + a_c)\exp(b_c \varepsilon_c^{ch}) - a_c \exp(-2 b_c \varepsilon_t^{ch})\right] \qquad (9)$$

$$d_t = 1 - \frac{1}{2 + a_t}\left[2(1 + a_t)\exp(-b_t \varepsilon_t^{ck}) - a_t \exp(-2 b_t \varepsilon_t^{ck})\right] \qquad (10)$$

Coefficients $b_c$ and $b_t$ can be obtained from Eq. (11) and coefficients $a_c = 7.87$ and $a_t = 1$.

$$b_c = \frac{f_{co} l_{eq}}{G_{ch}}\left(1 + \frac{a_c}{2}\right) \qquad \qquad b_t = \frac{f_{t0} l_{eq}}{G_F}\left(1 + \frac{a_t}{2}\right) \qquad (11)$$

The parameters based on failure criteria used in FE analysis is mentioned in Table 1.

Table 1
Parameters used for failure criteria of CDP model (Vermeer and de Borst, 1984)

| $K_c$ | $\Psi$ (º) | $f_{bo}/f_{co}$ | $\varepsilon$ |
|---|---|---|---|
| 0.70 | 32 | 1.16 | 0.1 |

### 2.4.2 Steel

Two different idealizations, shown in Figures. 2 (a) and (b), are commonly used in FE modelling of reinforcement depending on the desired level of accuracy. The first idealization neglects the strength increase due to strain hardening as shown in Figure 2 (a). In several instances it is necessary to evaluate the steel stress at strains higher than yield to more accurately assess the strength of members' at large deformations. In this case more accurate idealizations which account for the strain hardening effect are required as shown in Figure 2(b (Limkatanyu and Spacone, 2003). In the present analysis elasto-plastic material model is used.
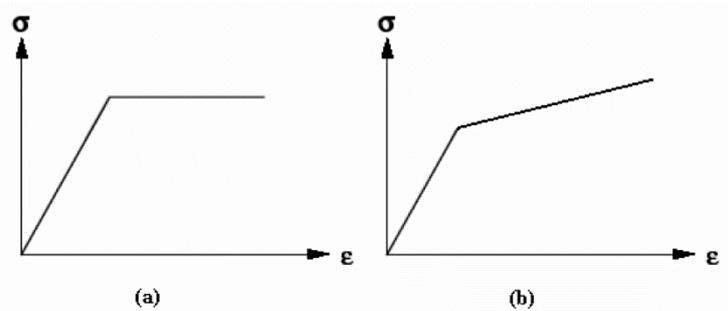


Fig. 2. Idealizations of the steel stress-strain curves of steel reinforcement (a) linear elastic, perfectly plastic and (b) elasto-plastic or bilinear (Limkatanyu and Spacone, 2003).
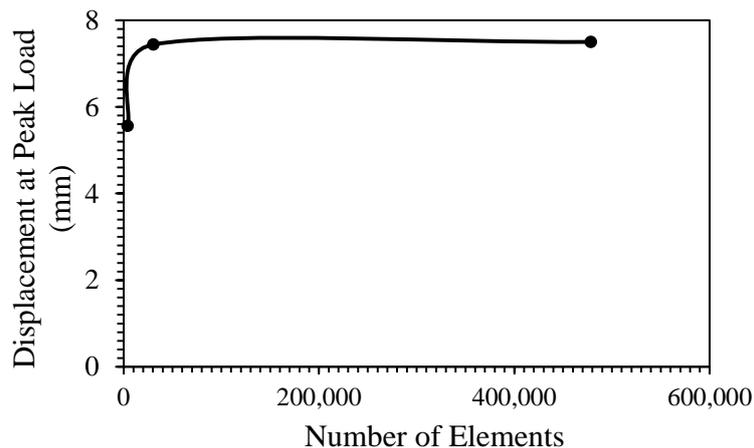


Fig. 3. Mid span deflection of beam at peak load Vs number of elements

### 2.4.3 Application of load

Reaction force between contact surface of the beam or column and loading plate is considered as the stiffness force i.e., static load of the beam or column. Load is evaluated by applying downward loads or displacements. Load is gradually increased by applying a downward vertical displacement at the midpoint of beam or top of the column. The maximum load

which the structure can sustain is measured and identified as the maximum capacity of the member.

### 2.5      *Mesh sensitivity analysis for static load*

Mesh convergence studies is conducted to determine the optimum FE mesh size that provides relatively accurate solution with low computational time. To do so, the RC beam mentioned in Section 3.2.2 with 8 mm shear reinforcement at 150 mm c/c is considered. Three type of mesh sizes 50 mm, 25 mm and 10 mm are used here to find out the optimum mesh size.

It is observed from Figure 3 that both 25 mm and 10 mm mesh size provide very close displacement value at peak load. But, 10 mm mesh size require larger number of elements for analysis as a result computation time increases approx. by 20 times than 25 mm mesh size. Hence, mesh size of 25 mm is considered as optimum for static analysis.

## 3.      Validation of proposed method

Three case studies are investigated for validation of proposed FE model and in each case the capability of model in specific condition is evaluated. In the first case, FE model is evaluated against different stages of loading on RC beam comparing with theoretical result. In the second case, FE model is evaluated in condition of stirrup change against analytical results and the test results of Saatci (2007). In the third case, tie bar changes of an RC column are considered for further evaluation of the proposed FE method against analytical results. In the final case, a frame is validated against test results of Güner (2008) under monotonic loading.

### 3.1.1      *Case study I: validation of FE model with gradually increasing static load on RC beam*

In this case study proposed FE method is checked by gradually increasing static load on RC beam to predict behavior in all load stages up to failure adopted from (Darwin et al. 2016). FE results are compared with those obtained from general mechanics of reinforced concrete structures. Figure 4 (a) shows the details of RC beam. This beam is supported by two steel plates and loaded at center by another steel plate. The dimension of supporting and loading plate is 25 x 150 x 250 mm. The beam has no shear reinforcement. The clear cover of the beam from center of flexure reinforcement is 50 mm.
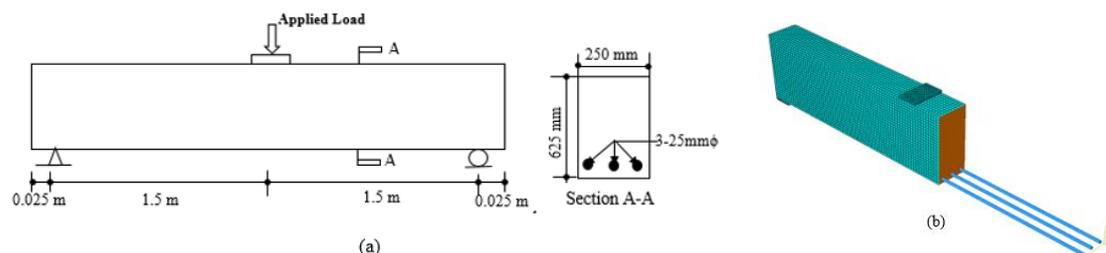


Fig. 4.  (a) Geometry details and (b) FE model of RC beam.

Tables 2 and 3 indicate the material properties of reinforcement and concrete used in present FE analysis. Nonlinear properties of concrete are evaluated using CDP model.

Table 2
Properties of reinforcing bar

| Bar Size (mm) | Density (kg/m$^3$) | Area (mm$^2$) | Yield strain x10$^{-3}$ (mm/mm) | Yield stress (MPa) | Ultimate strength (MPa) | Young's Modulus (GPa) | Ultimate strain x10$^{-3}$ (mm/mm) |
|---|---|---|---|---|---|---|---|
| 20 | 7800 | 510 | 2.07 | 414 | 620 | 200 | 80 |

Table 3
Properties of concrete

| Density, $\rho$ (kg/m³) | Modulus of elasticity, E (GPa) | Ultimate stress (MPa) | Ultimate strain x $10^{-3}$ (mm/mm) | Modulus of rupture (MPa) |
|---|---|---|---|---|
| 2400 | 24.69 | 28 | 3.08 | 3.27 |

### 3.1.2   Response of RC beam under different stages of loading

a) **Stress elastic and section uncracked:** At low loads, as long as the maximum tensile stress in the concrete is smaller than the modulus of rupture, the entire concrete is effective in resisting stress.  In addition, the reinforcement is deformed the same amount as the adjacent concrete. At this stage, all stresses in concrete are proportional to stains. As a result, no tension cracks have developed. At this stage of analysis, transformed section as shown in Figure 5 (b) is used.

Modular ratio, $n = E_s/E_c = 8$ and moment of inertia of transformed section, $I = 5.76 \times 10^9$ mm⁴.

From ABAQUS (2014) results, it was found that up to 99.8 kN load, there is no flexural crack. The calculated moment under 99.8 kN load is, $M = \frac{PL}{4} = 74.9$  kN-m
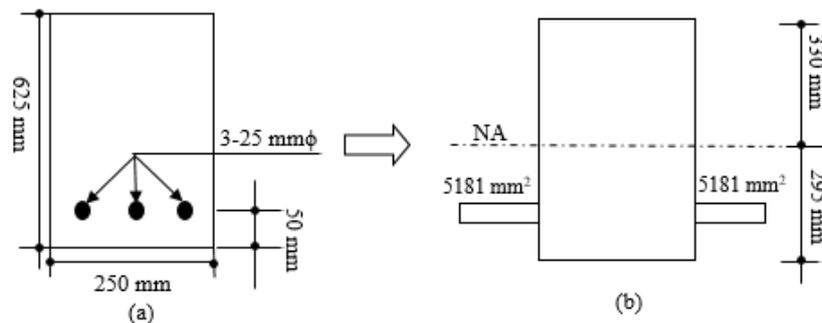


Fig. 5. (a) cross section and (b) transformed section of the RC beam.

So, tensile stress at bottom fiber of concrete is, $\sigma_t = \frac{My}{I} = 3.34$ MPa which is almost equal to the modulus of rupture of concrete (3.27 MPa). So, theoretically no cracks have been developed at bottom fiber of RC beam. The stress block across the beam remains linear.
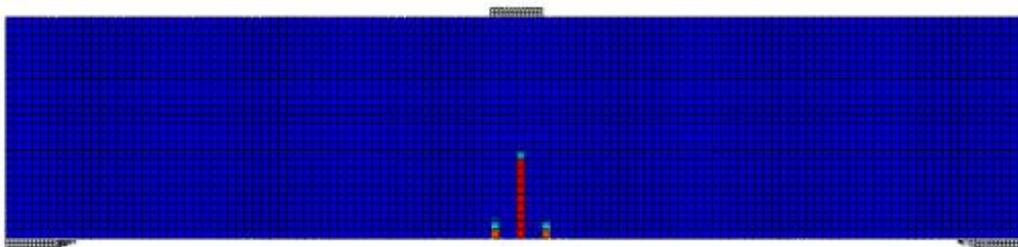


Fig. 6. Crack pattern of RC beam at 107.8 kN load (elastic, cracked).

b) **Stress elastic and section cracked:** When the load is further increased, the tensile strength of the concrete is soon reached and at this stage tension cracks develop. These cracks propagate quickly upward or close to the level of neutral plane, which in turn shifts upward with progressive cracking.  It is found that under 107.8 kN concentrated load first flexural cracks is appeared at the centre of the beam.  The calculated moment at midspan of the beam under 107.8 kN concentrated load is 80.9 kN-m ($M = \frac{PL}{4}$ ).

So, tensile stress at bottom fiber of concrete is, $\sigma_t = \frac{My}{I} = 3.61$ MPa which is greater than modulus of rupture of concrete (3.27 MPa). So, theoretically cracks have been developed at bottom fiber of RC beam. The stress block across the beam remains linear. The crack pattern of the analyzed beam under 107.8 kN concentrated load at center of beam is shown in Figure 6. Moreover, it is also found that tensile stress in concrete decrease due to development of tension crack at the bottom of concrete.

At moderate loads, if the concrete stresses do not exceed approximately half of $f_c'$ stresses and strains continue to be closely proportional. At this stage it is assumed that tension cracks have progressed all the way to the neutral axis. As per ACI 318-11, the depth of stress block is "kd" $(where, \mathrm{k} = \sqrt{(\rho n)^2 + 2\rho n} - \rho n = 0.332)$. So, depth of stress block "kd" is 191 mm.

The compressive stress equal to 0.45 $f_c'$ (12.60 MPa) at top face of beam is produced by the moment "$M_e$". So, $M_e = \frac{1}{2} f_c \mathrm{kjbd}^2 = 154$ kN $-$ m.

This moment will be produced when concentrated load at midspan of beam is 205 kN (P = $\frac{4M}{L}$). The stress distribution and crack pattern under 205 kN concentrated load at mid-span of beam is shown in Figure 7. Stress across the beam remains linear and depth of the stress block obtained from FE analysis is 192.5 mm which is almost similar to the theoretical value of 191 mm.
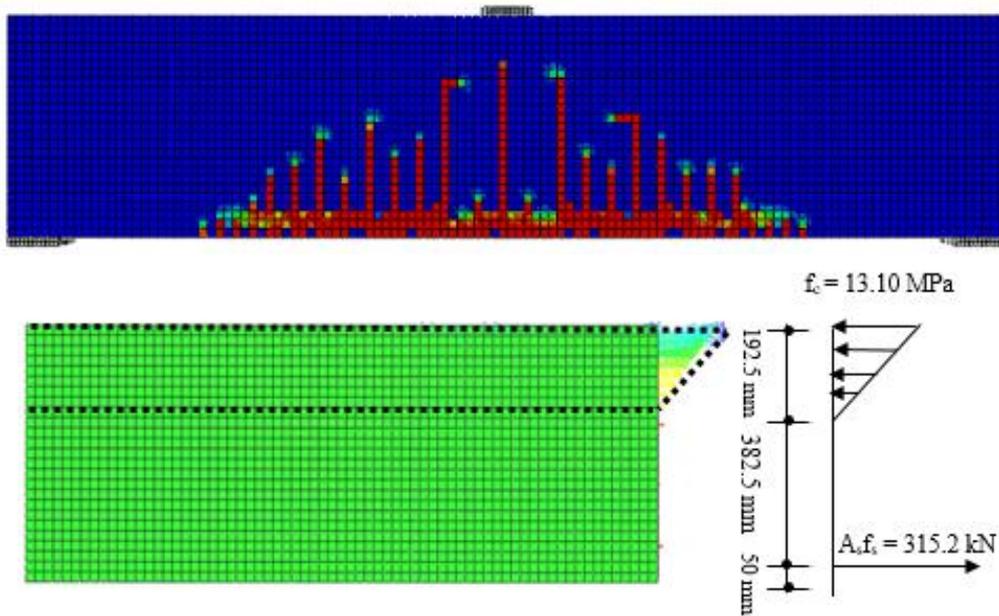


Fig. 7.  (a) crack pattern and (b) stress distribution at mid-span under 205 kN load.

c) *Loading which produces nominal moment (section become plastic and cracked):* When the load is still further increased, stresses and strains rise correspondingly and are no longer proportional. Then linear procedure is not applicable for stress calculation. As per ACI 318-11, the stress block depth, $a = \frac{\rho d f_y}{0.85 f_c'} = 103$ mm, so $c = \frac{a}{\beta_1} = 121$ mm. Corresponding nominal moment, $M_n$ is

$$M_n = A_s f_y \left( d - \frac{a}{2} \right) = 336 \text{ kN} - \text{m}$$

This moment will be produced when concentrated load at midspan of beam is $P = \frac{4M}{L} =$ 448 kN. The crack pattern and stress distribution under 448 kN concentrated load at midspan of beam are shown in Figure 8.
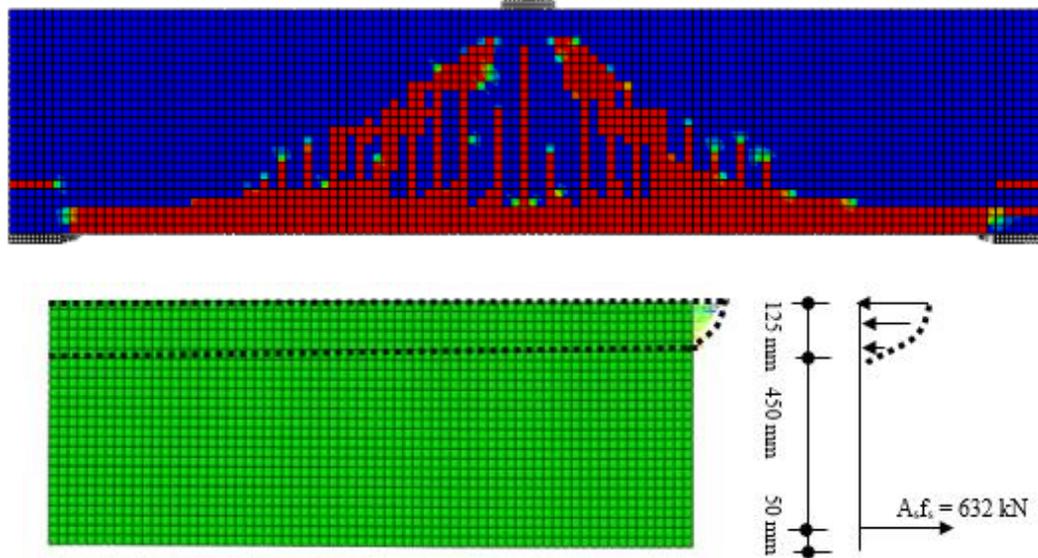


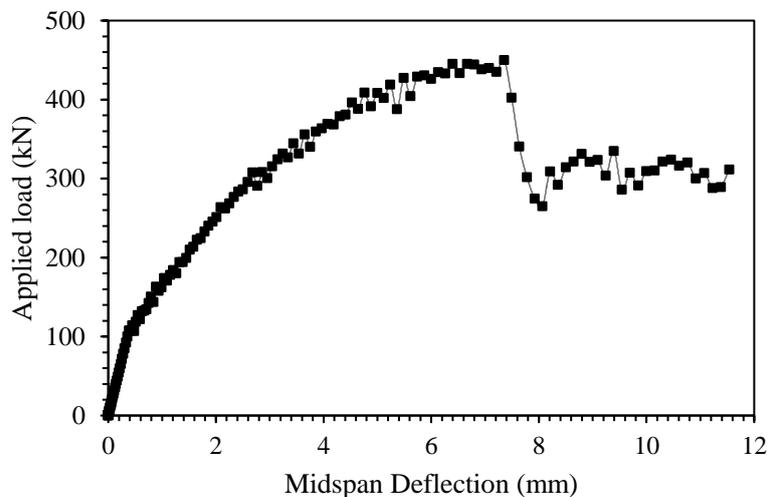Fig. 8. (a) Crack pattern and (b) stress distribution at mid-span under 448 kN load.



Fig. 9. Load deflection of simulated RC beam.

Load-midspan deflection plot of RC beam is shown in Figure 9. From load deflection plot, it is observed that the initial portion of the curve under service load of 99.8 kN is approximately elastic. Up to 205 kN load, the stress and strain remain linear. The simulated beam is failed under 450 kN peak load.

### 3.1.3    Case study II: Validation of FE model in condition of stirrup change

In this case study, the proposed FE method is validated based on different stirrups configurations. Initially, two RC beams have been validated against analytical result with similar boundary conditions and geometry, but with different numbers of stirrups. Likewise, another three RC beams have been validated against the test results of Saatci (2007) with different numbers of stirrups.

### 3.1.4    RC beams with and without stirrup under static load verified with analytical results

Shear reinforcements are varied for the two beams identified as SS0, has no shear reinforcement and SS1, has 10 mm diameter shear reinforcement spaced at 150 mm c/c to understand their effects on failure type. The beams are supported by two steel plates and loaded at two points by another two-steel plates. The dimension of both the supporting and loading plate is 25 mm x 50 mm x 250 mm. Both beams are reinforced by two no. 29 mm diameter reinforcing bars as bottom flexural reinforcement. Details of the RC beam with FE model is shown in Figure 10. Clear cover of beam is 37.5 mm.
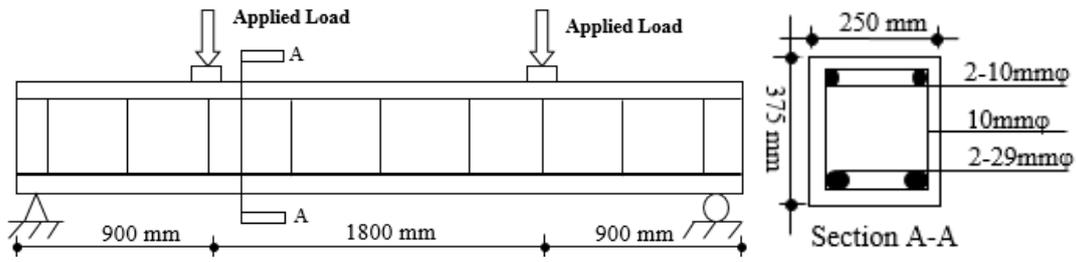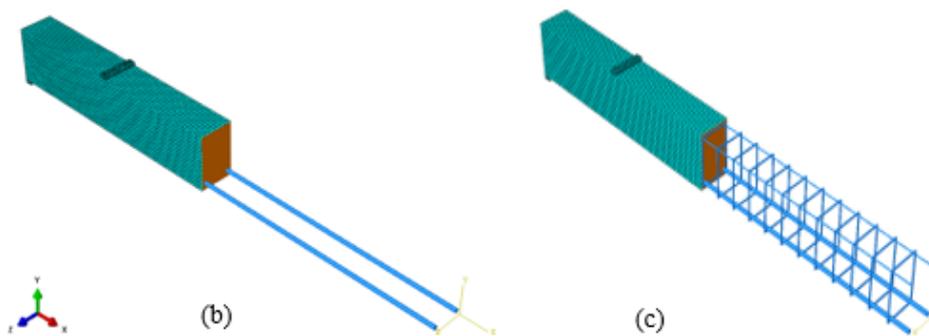


Fig. 10(a).  Geometry details.



Fig. 10(b).  FE model of SS0 and (c) FE model of SS1 RC beam.

Table 4 indicates the material properties of reinforcements.  Compressive strength of concrete is 37.5 MPa.

Table 4
Properties of reinforcing bars

| Bar Size (mm) | Area (mm$^2$) | Density P (kg/m$^3$) | Yield strain x10$^{-3}$ (mm/mm) | Yield stress (MPa) | Ultimate strength (MPa) | Young's Modulus (MPa) | Ultimate strain x10$^{-3}$ (mm/mm) |
|---|---|---|---|---|---|---|---|
| 29 | 661 | 7800 | 1.72 | 345 | 448 | 200000 | 80 |
| 10 | 78 | | | | | | |

The failure patterns of RC beam are basically two types, one is shear failure and another is flexural failure. If the flexural capacity of a beam is larger than the shear capacity, the beam is failed by shear failure. Shear capacity of a beam is provided by concrete of beam itself and additional shear reinforcement. The nominal moment capacity of the beam due to flexural reinforcement as per ACI 318-11 (2011) is, $M_n = A_s f_y \left(d - \frac{a}{2}\right) = 150$ kN-m [a = $\frac{A_s f_y}{0.85 f_c' b}$ = 55.25 mm]  and corresponding applied load is $P_n = \frac{4M}{L} = 166$ kN.

For the beam with shear reinforcement (SS1), shear capacity is provided by both shear reinforcement and concrete itself. Total shear capacity of SS1 beam as per ACI 318-11 (2011) is, $V_n = V_c + V_s = 2\sqrt{f_c' \text{ (psi)}} \, b_w d + \frac{A_v f_y d}{s} = 288.54$ kN
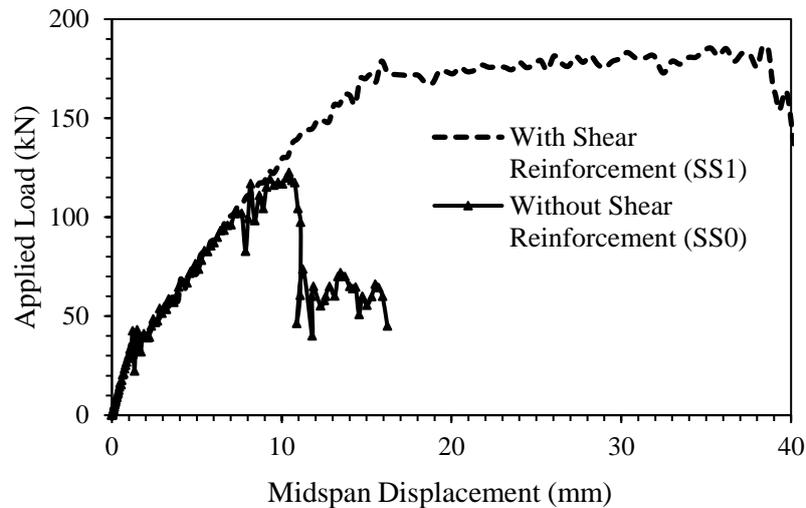
Fig. 11. Load-deflection plot of simulated RC beam with and without shear reinforcement

Load–midspan deflection results of the RC specimens under two different stirrup conditions are shown in Figure 11. It is seen from the FE analysis that the maximum flexure capacity of the RC beam with 10 mm diameter shear reinforcement (SS1) is 184 kN which is less than 288.54 kN shear capacity of this beam obtained from analytical result. So, SS1 beam has failed in flexure.

Shear capacity of beam without shear reinforcement (SS0) as per ACI 318-11 (2011) is, $V_n = V_c = 2\sqrt{f_c{}'}$ (psi)$b_w d = 90.8$ kN which is provided by concrete only. It is also observed from FE analysis that the flexure capacity of SS0 beam is 122 kN which is greater than the shear capacity of SS0 beam. So, this beam has failed in shear. In general, FE results have reasonable agreement with analytical data.

### 3.1.5    RC beams with varying stirrup verified against experimental results

In the present section experimental load-deflection plots of RC beams tested by Saatci (2007) are considered for validation. Three simply supported RC beams with identical longitudinal reinforcement and varying shear reinforcement were used by Saatci (2007). All beams had the same amount of longitudinal reinforcement: two No. 30 (area = 707 mm$^2$) steel bars placed with 37.5 mm clear cover at the bottom and top of the beam. The details of the tested RC beam are presented in Figure 12.
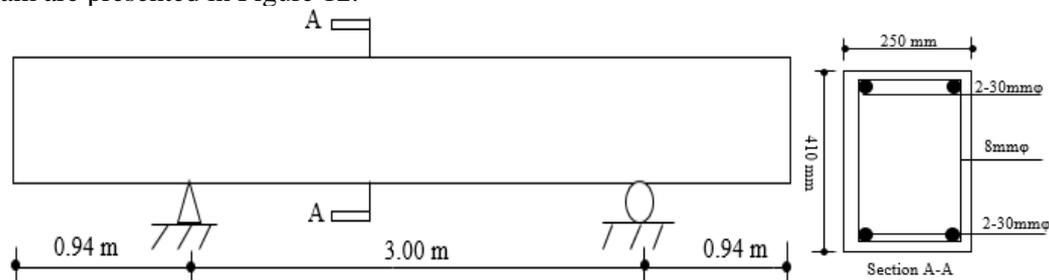


Fig. 12. Details of RC beam tested beam by Saatci (2007).

Shear reinforcements were varied for different beams to understand their effects on failure behaviour of beam. The type of shear reinforcement used in these tests were 8 mm reinforcing bar (area = 50 mm$^2$). Details of shear reinforcement are presented in Table 5.

Table 5
Transverse reinforcement ratios and stirrup spacing for beams

| Specimen | Ratio of shear reinforcement | Spacing of shear reinforcement (mm) |
|---|---|---|
| MS0 | no shear reinforcement | - |
| MS1 | 8 mm diameter shear reinforcement (0.1%) | 300 |
| MS2 | 8 mm diameter shear reinforcement (0.2%) | 150 |

The concrete compressive strength of the tested beam was 50 MPa. Properties of reinforcing bars are given in Table 6.

Table 6
Properties of reinforcing bar

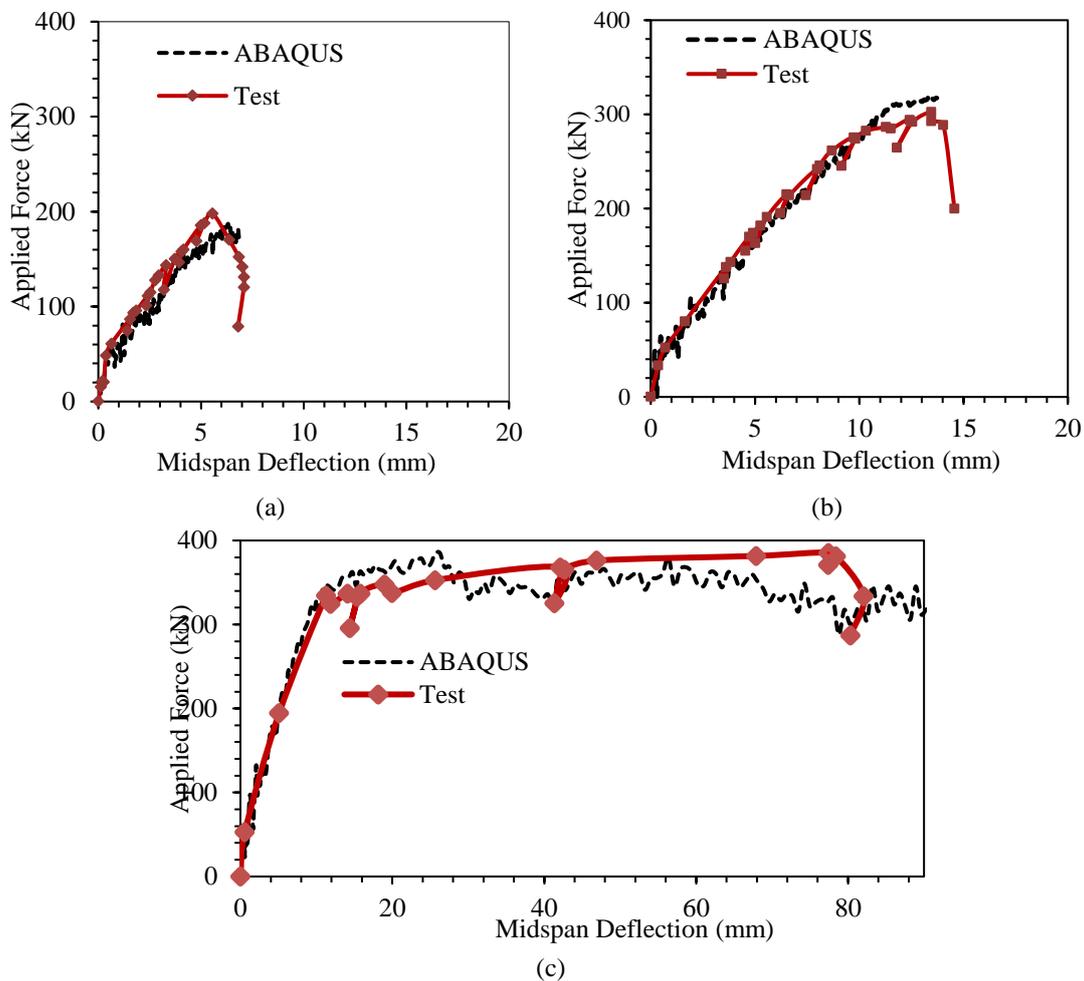| Bar Size (mm) | Area (mm²) | Yield Strain x10⁻³ (mm/mm) | Yield Stress (MPa) | Ultimate Strength (MPa) | Young's Modulus (GPa) | Ultimate Strain x10⁻³ (mm/mm) |
|---|---|---|---|---|---|---|
| 30 | 707 | 2.5 | 464 | 690 | 200 | 80 |
| 8 | 50 | 4.9 | 572 | 623 | 117 | 50 |



(a)                              (b)

(c)

Fig. 13.  Load Vs deflection plots of beams (a) MS0, (b) MS1 and (c) MS2.

Figures 13 (a) to (c) show the load versus mid-span deflection plots of RC beam found from experiment and FE analyses with three different stirrups spacing as mentioned in Table 5. The displacement is applied at mid-span of the beams by loading pad (bearing plate) and analyses have been executed by ABAQUS/Explicit (2014). Reaction force between contact surface of the beam and loading plate is considered as the stiffness force i.e., static load of the beam. Undulation is observed in both the experimental as well as in numerical load vs. deflection

plots because of the vibration created by tension crack during analysis. This phenomenon is also observed during flexural test of any RC beam.

The FE response of all the beams is found to be very similar to the actual response viewed in the test. From Figures. 13 (a) to (b), it is also observed that the flexure capacity and displacement are increasing from beam MS0 to MS1 due to the increase of stirrup ratio.

### 3.1.6    Case study III: Validation of FE model in condition of tie bars change

In this case study, the proposed FE method is validated based on different ties configurations of two RC columns, one with tie (TS1) and another without tie (TS0). Both the columns are of 3.25 m long with cross-section of 400 mm x 400 mm with fixed base. The columns are reinforced by eight no. 35 mm diameter reinforcing bars as main reinforcement.  The clear cover from the center of main reinforcement to the outer surface of columns is 62.5 mm. In order to have deep insight of confinement effect and failure behavior, tie bars are varied for the two columns.  The type of tie bar used in this analysis are 12 mm reinforcing bar (area = 113 mm$^2$).  Properties of reinforcing bars is mentioned in Table 2 and compressive strength of concrete used is 43 MPa.  Figure 14 shows the geometry details of TS1 column and FE model of TS0 and TS1 column.
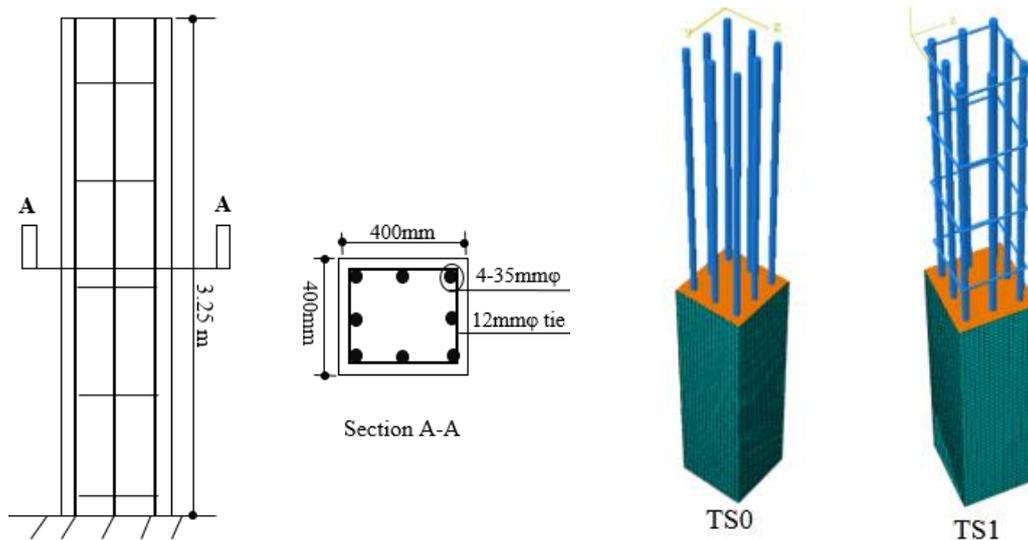


Fig. 14.  (a) Geometry details and (b) FE model of RC column.

Nominal capacity of axially loaded RC column is as per ACI Code (ACI 318-11, 2011),
$$P_N = 0.85 f_c' \left( A_g - A_{st} \right) + f_y A_{st} = 8753 \text{ kN}$$

$P_N$ depends on concrete compressive strength $(f_c')$, yield strength $(f_y)$, of longitudinal reinforcement, gross cross-sectional area of column $(A_g)$ and area of longitudinal reinforcement $(A_{st})$. During numerical analyses in ABAQUS (2014) axial load is applied at top of the columns as downward displacement using 25 mm thick steel plate.  While applying the load, top of the columns is allowed to move downward where base of the columns is fixed. Mass scaling technique is used to reduce the time period of analysis.  The reaction force between contact surface of the column and loading plate is considered as the stiffness force i.e., axial load of the column. Axial force versus axial displacement plots of both the columns, without tie bar (TS0) and with 10 mm tie bars spaced at 400 mm c/c (TS1), obtained from present FE analyses is shown in Figure 15.
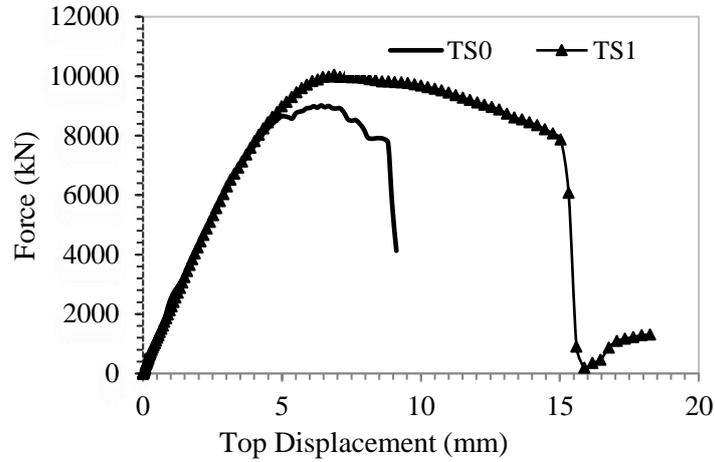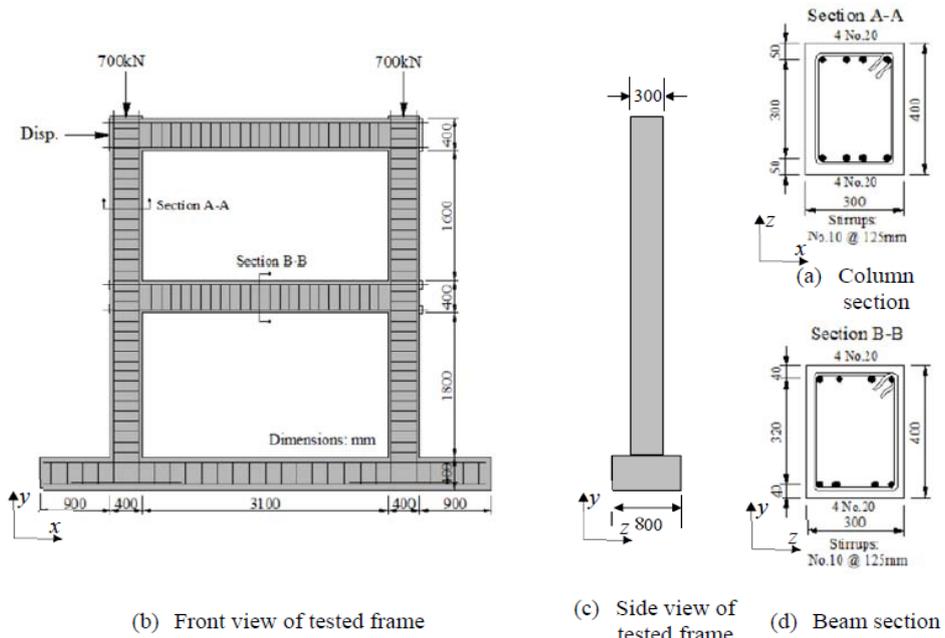
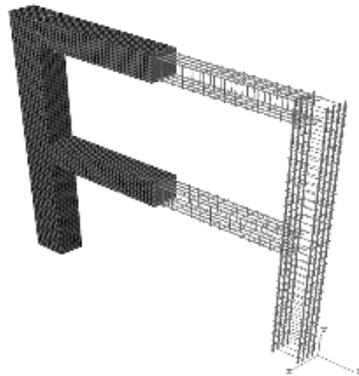Fig. 15.  Load displacement plots of RC columns TS0 and TS1.



Fig. 16.  Details of the RC frame experiment (Güner, 2008) and FE model.

It is observed from load displacement that axial capacity of TS0 and TS1 columns obtained from FE analysis are 9018 and 10047 kN respectively. Moreover, axial displacement of TS0 and TS1 column at failure are found to be 8.97 and 18.24 mm respectively. TS1 column shows larger displacements and higher capacity due to the presence of tie bars around the

longitudinal reinforcement.  So, it can be concluded that inclusion of tie bar can increase the axial capacity as well as axial displacement of any RC column.

*3.1.7    Case study IV: Validation of FE model of RC frame under monotonic load*

Numerical simulation of an RC frame under monotonic loading is validated comparing with the test results obtained from Güner (2008). The tested RC frame was two-storied single span planar frame. Front and side views of the tested frame are displayed in Figures. 16 (b) and (c), respectively. Cross sectional dimensions of columns and beams are exhibited in Figures. 16 (a) and (d), respectively. All the dimensions used in Figure 15 were in mm. Figure 16 (b) shows that both columns are loaded with 700 kN constant forces that pushing consisted in imposing a displacement law to the top left joint. Noticeably, since there were no distributed forces acting on the beams, there was no cracking prior to the lateral pushing. Properties of reinforcing bar obtained from Güner (2008) is presented in Table 7 and 28 MPa concrete was used by Güner (2008).

Table 7
Properties of reinforcements

| Bar dia (mm) | Area (mm$^2$) | Yield stress (MPa) | Ultimate stress (MPa) | Modulus of elasticity (GPa) | Strain at hardening strain x $10^{-3}$ (mm/mm) | Ultimate strain x $10^{-3}$ (mm/mm) |
|---|---|---|---|---|---|---|
| 20 | 314 | 418 | 596 | 193 | 9.5 | 67 |
| 10 | 78 | 454 | 640 | 200 | 9.5 | 67 |

During numerical analysis by ABAQUS (2014), the loads are applied in two steps. In first step, initial constant forces of 700 MPa is applied on top end of the columns as linearly increasing load to produce initial stress state.  In second step, a gradually increasing lateral displacement is applied at top left corner of the column. During the application of load, base of the columns is kept fixed.  Lateral force versus deflection plot of top left corner of the frame obtained from FE analysis is shown in Figure 17.
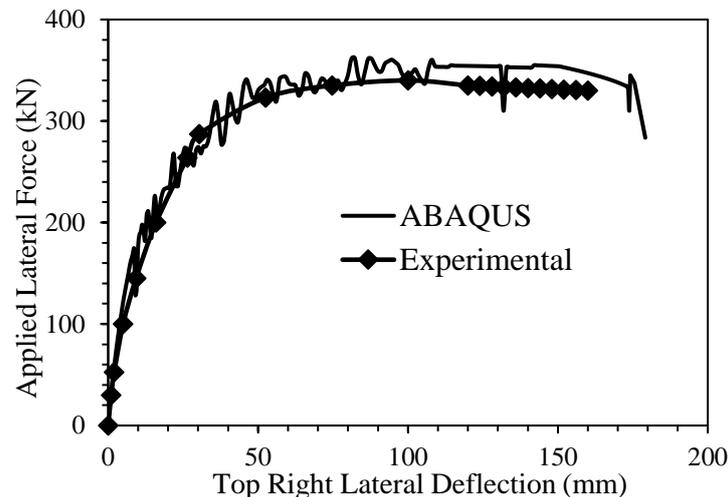
Fig. 17.  Lateral force vs deflection of simulated RC frame with test result of Güner (2008).

From load deflection plot, the peak lateral load obtained from FE analysis is 350 kN whereas the experimental frame sustained upto 340 kN load. The differences obtained in peak lateral forces between the experimental and present numerical analysis is 3% which is reasonable. Undulation has been observed in load deflection plot because the beam is vibrated by tension crack during analysis.

*3.1.8    Crack patterns and damage*

The crack patterns and damage obtained from the test is compared with present FE analysis. Figure 18 (a) presents the crack patterns of RC frame tested by Güner (2008) and Figure 18 (b) presents the tension damage of the frame obtained from FE analysis using CDP model. The crack patterns obtained from FE analysis conform reasonably well with the test result of Güner (2008).
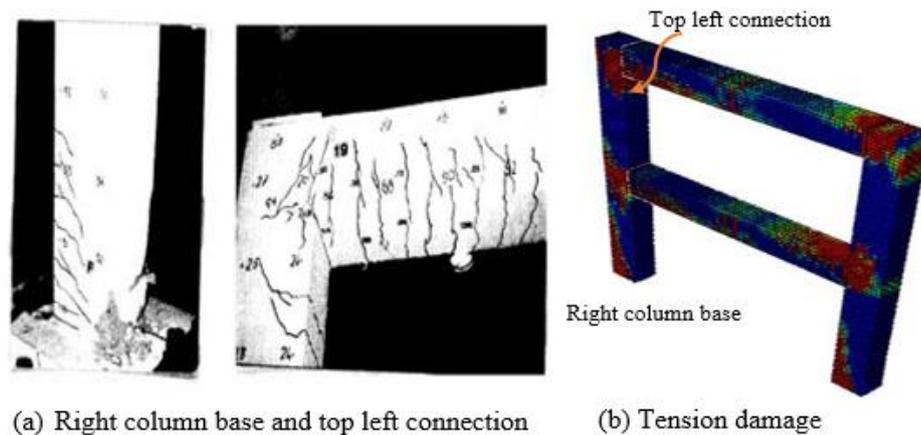


(a) Right column base and top left connection      (b) Tension damage

Fig. 18. Damage pattern of RC frame (a) experimental (Güner, 2008) and (b) simulated.

## 4.      Conclusions

From limited study of this current research works, following conclusions can be drawn:

−   Numerical modelling of RC beam, column and frame are done successfully against static load using FE software ABAQUS (2014) based on nonlinear FE method. The stress distributions, crack patterns, failure type and load carrying capacity of the RC beam, column and frame under static load obtained from present numerical analyses are shown a good correlation with the theoretical and experimental results.
−   FE model is validated with gradually increasing static load on RC beam to predict and compare different stages of loading. FE result shows good agreement with the theoretical result in each loading stages, i.e., a) stress elastic and section uncracked, b) stress elastic and section cracked, and c) loading which produce nominal moment, Mn (stress become plastic).
−   FE model of RC beams with similar boundary conditions and geometry but with different numbers of stirrups have been verified against theoretical as well as test result of Saatci (2007) using the proposed method to understand their effects on flexure capacity and failure behavior of beam. FE analyses shows that with the increase of stirrup percentage, the load carrying capacity and ductility of the column increase. Besides, it is observed that beam without shear reinforcement fails in shear and beam with adequate shear reinforcement fails due to flexure.
−   FE model of RC columns with similar boundary conditions and geometry but with different numbers of ties have been checked against theoretical result using the proposed method to have deep insight of confinement effect and failure behavior. FE analyses shows that inclusion of tie bar can increase the axial capacity as well as axial displacement of any RC column.
−   FE simulation of RC frame under monotonic loading is verified by comparing with the test results obtained from Güner (2008). Good correlation in load displacement plot between the FE analysis and test result is found. Moreover, crack patterns of the RC

frame from nonlinear FE analyses using the CDP model of ABAQUS (2014) conform reasonably well to the cracks and damage patterns observed in the tests.

**References**

ABAQUS (2014), ABAQUS version 6.14, ABAQUS Analysis user's manual.

Building Code Requirements for Reinforced Concrete (2011). American Concrete Institute, (ACI 318-11), Detroit.

Buyukozturk, O., (1977). Nonlinear analysis of reinforced concrete structures. Comput Struct 7(1), 149–156.

CEB-FIP (2010). Model Code 2010. Thomas Telford, London.

Darwin, D., Dolan, C. W., & Nilson, A. H. (2016). Design of concrete structures. New York, NY, USA, McGraw-Hill Education.

Guner, S. (2008). Performance assessment of shear-critical reinforced concrete plane frames. PhD thesis, Civil Engineering Department, University of Toronto, Canada.

Hordijk, D. A. (1992). Tensile and tensile fatigue behaviour of concrete; experiments, modelling and analyses. Heron, 37(1).

Hutton, D.V., Wu J., (2004). Fundamentals of finite element analysis. McGraw-Hill, New York.

Kingery C. N., Bulmash G. (1984). Technical report ARBRL-TR-02555: Air blast parameters from TNT spherical air burst and hemispherical burst. AD-B082 713, U.S. Army Ballistic Research Laboratory, Aberdeen Proving Ground, MD.

Krätzig, W. B., & Pölling, R. (2004). An elasto-plastic damage model for reinforced concrete with minimum number of material parameters. Computers & structures, 82(15-16), 1201-1215.

Lubliner, J., Oliver, J., Oller, S., & Onate, E. (1989). A plastic-damage model for concrete. International Journal of solids and structures, 25(3), 299-326.

Lee, J., & Fenves, G. L. (1998). Plastic-damage model for cyclic loading of concrete structures. Journal of engineering mechanics, 124(8), 892-900.

Limkatanyu, S., & Spacone, E. (2003). Effects of reinforcement slippage on the non-linear response under cyclic loadings of RC frame structures, Earthquake engineering & structural dynamics, 32(15), 2407-2424.

Nilson, A. H., Darwin, D., & Dolan, C. W. (2004). Design of concrete structures. 18th ed., Boston, McGraw-Hill Higher Education.

Oller, S. (2014). Nonlinear dynamics, international centre for numerical methods in engineering. Technical University of Catalonia.

Richard, B., Frau, A., Ma, A., Loiseau, O., Giry, C., Ragueneau, F., (2015). Experimental and numerical study of a half-scaled reinforced concrete building equipped with thermal break components subjected to seismic loading up to severe damage state. Eng Struct 92, 29–45.

Saatci, S., & Vecchio, F. J. (2009). Effects of shear mechanisms on impact behaviour of reinforced concrete beams. ACI Structural Journal, 106.

Tong, L., Liu, B., Zhao, X.L. (2017). Numerical study of fatigue behaviour of steel reinforced concrete (SRC) beams. Eng Fract Mech178, 477–496.

Vecchio, F.J., (1989). Nonlinear finite element analysis of reinforced concrete membranes. ACI Struct J 86(1), 26–35.

Vermeer, P. A., & De Borst, R. (1984). Non-associated plasticity for soils, concrete and rock. HERON, 29 (3).

Zhang F., Wu, C., Wang, H., Zhou, Y. (2015). Numerical simulation of concrete filled steel tube columns against BLAST loads. Thin Walled Struct 92, 82–92.